4. CONCLUSION

A bandwidth enhancement technique for designing of microstrip planar antenna is presented for broadband wireless communication. By shifting the off-set fed radiating patch from the center of dielectric substrate it is seen that a 115.5% enhancement in the operating band can be achieved. The proposed planar antenna with bandwidth enhancement technique is prototyped and it is found that the designed antenna without etching any slot/slit/parasitic element can achieve a fractional bandwidth of 146% ranging from 2.96 to 19GHz. The antenna also achieved a good gain and exhibited stable omni-directional radiation patterns. The attractive features of the proposed planar antenna such as simple structure, less expensive, small size makes it very suitable for numerous wireless communications applications.

ACKNOWLEDGMENT

This work was supported by the Deanship of Scientific Research (DSR) at King AbdulAziz University, Jeddah, Saudi Arabia under grant no. 3-135-35-RG.

REFERENCES

1. I.J. Bhal, Microstrip antennas, Artech House, Norwood, MA, 1980.
2. D.M. Pozar,Microstrip antennas, IEEE Proc 80 (1992), 79–91.
3. M.N. Shakib, M.T. Islam, and N. Misran, Stacked patch antenna with folded patch feed for ultra-wideband application, IET Microwave Antenna Propag 4 (2010), 1456–1461.
4. S.N. Ather and P.K. Singhal, Truncated rectangular microstrip antenna with H and U slot for broadband, Int J Eng Sci Technol 5 (2013), 114–118.
5. D. Pozar and B. Kaufman, Increasing the bandwidth of a microstrip antenna by proximity coupling, Electron Lett 23 (1987), 368–369.
6. S. Kaya and E. Y. Yuksel, Investigation of a compensated rectangular microstrip antenna with negative capacitor and negative inductor for bandwidth enhancement, IEEE Trans Antenna Propag 55 (2007), 1275–1282.
7. A.A. Deshmukh, A.R. Jain, and K.P. Ray, Broadband sectoral slot cut microstrip antenna, In National Conference on Communications, New Delhi, India, 2013.
8. J.-Y. Jan and J.-W. Su, Bandwidth enhancement of a printed wide-slot antenna with a rotated slot, IEEE Trans Antenna Propag 53 (2005), 2111–2114.
9. A. Dastranj and H. Abiri, Bandwidth enhancement of printed E-shaped slot antennas fed by CPW and microstrip line, IEEE Trans Antenna Propag 58 (2010), 1402–1407.
10. Y. Sung, Bandwidth enhancement of a microstrip line-fed printed wide-slot antenna with a parasitic center patch, IEEE Trans Antenna Propag 60 (2012), 1712–1716.
11. M. Ojaroudi, S. Yazdanifard, N. Ojaroudi, and M. Naser-Moghaddasi, Small square monopole antenna with enhanced bandwidth by using inverted T-shaped slot and conductor backed plane, IEEE Trans Antenna Propag 59 (2011), 670–674.
12. R. Azim, M.T. Islam, and N. Misran, Microstrip line-fed printed planar monopole antenna for UWB applications, Arab J Sci Eng 38 (2013), 2415–2422.
13. R. Azim, M.T. Islam, and N. Misran, Printed circular disc compact planar antenna for UWB applications, Telecommun Syst 52 (2013), 1171–1177.
14. N. Prombutr, P. Kirawanich, and P. Akkaraekthalin, Bandwidth enhancement of UWB microstrip antenna with a modified ground plane, Int J Microw Sci Technol 2009 (2009), 1–7.
15. R. Azim, M.T. Islam, and N. Misran, Design of a planar UWB antenna with new band enhancement technique, Appl Comput Electrom Soc J 26 (2011), 856–862.
16. L.M. Si, H. Sun, Y. Yuan, and X. Lv, CPW-fed com-pact planar UWB antenna with circular disc and spiral split ring resonators, In Progress in Electromagnetics Research Symposium, Beijing, China, 2009, pp. 502–505.
17. M.T. Islam and R. Azim, Recent trends in printed ultra-wideband (UWB) antennas, InTechOpen, 2013.
18. Available at: http://www.satimo.com/
19. L. Liu, Y.F. Weng, S.W. Cheung, T.I. Yuk, and L.J. Foged, Modeling of cable for measurements of small monopole antennas, In Loughborough Antennas Propagation Conference, Loughborough, UK, 2011.
20. N. Ojaroudi, Microstrip monopole antenna with dual bandstop function for UWB applications, Microwave Opt Technol Lett 56 (2014), 818–822.

GPS/WLAN OPEN-SLOT ANTENNA WITH A STICKER-LIKE FEED SUBSTRATE FOR THE METAL-CASING SMARTPHONE

Kin-Lu Wong,[1] Yu-Ching Wu,[1] Che-Chi Wan,[1] and Wei-Yu Li[2]

[1] Department of Electrical Engineering, National Sun Yat-Sen University, Kaohsiung 80424, Taiwan; Corresponding author: wongkl@ema.ee.nsysu.edu.tw

[2] Information and Communications Research Laboratories, Industrial Technology Research Institute, Hsinchu 31040, Taiwan

Received 30 August 2015

ABSTRACT: *A multiband open-slot antenna formed by placing a sticker-like feed substrate (can also be a flexible printed-circuit board) with the microstrip feedline and circuit elements disposed thereon onto a simple linear open slot embedded in the metal casing of the modern smartphone is presented. The proposed design provides a simple and convenient method in feeding an open-slot antenna with multiband operation for the smartphone with a metal casing thereof having either a planar or smoothly curved surface. The linear slot has a short length of 23.5 mm and a narrow width of 1.5 mm and can be located 8 mm to the top or bottom edge of the metal casing. The linear slot is hence close to the short edge of the metal casing and will not be covered by the display panel therein. Such an open-slot antenna is simple in structure and small in size, yet it can cover the GPS operation at 1.575 GHz and the 2.4/5.2/5.8-GHz WLAN operation. The microstrip feedline printed on the feed substrate excites the open slot embedded in the metal casing, and the multiband (1.575/2.4/5.2/5.8 GHz) operation is obtained by the circuit elements disposed on the feed substrate. The circuit elements include a shunt capacitor loaded across the open slot and a parallel capacitor added to the microstrip feedline. Working principle of the applied circuit elements in obtaining the multiband operation is addressed. The antenna is also fabricated, and the experimental results are presented and discussed.* © 2016 Wiley Periodicals, Inc. Microwave Opt Technol Lett 58:1226–1232, 2016; View this article online at wileyonlinelibrary.com. DOI 10.1002/mop.29773

Key words: *mobile antennas; smartphone antennas; open-slot antennas; WLAN antennas; GPS antennas; multiband antennas; sticker-like feed substrate*

1. INTRODUCTION

Owing to its small size with a quarter-wavelength resonant structure and furthermore capable of integration with the surrounding metallic plate and electronic elements nearby [1–5], the open-slot antenna has been very attractive for applications in the metal-casing smartphone [6–11]. Such an open-slot antenna is suitable to have its open slot embedded in the metal casing of the smartphone. However, since the modern smartphone is generally equipped with a large display panel, it is demanded that the open slot be disposed close to the short edge (top or bottom edge) of the smartphone. In this case, the open slot will not be covered by the display panel, and acceptable performance of the

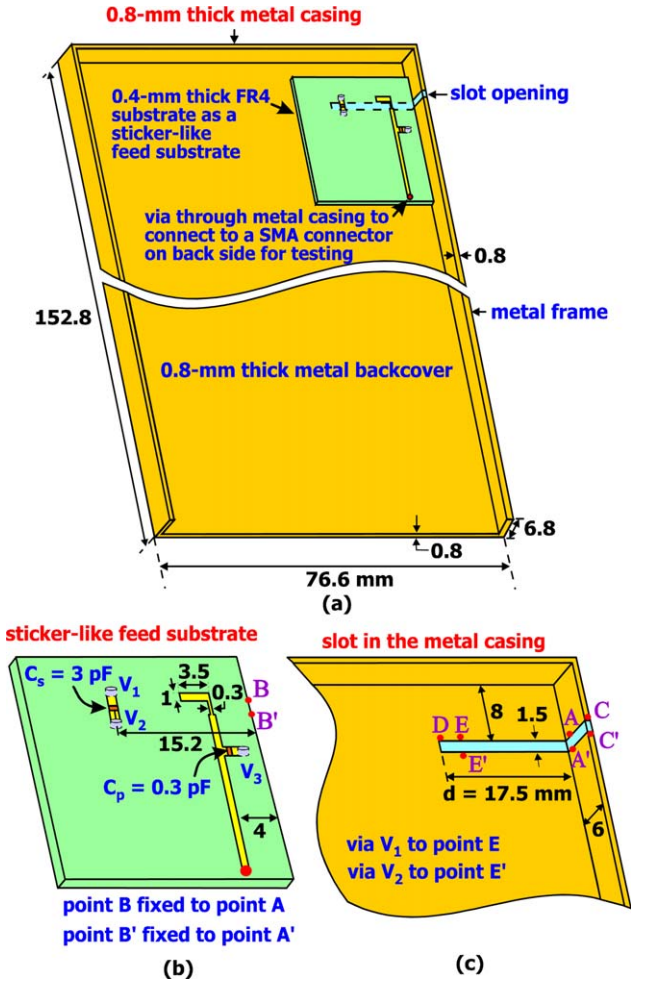

Figure 1 (a) Geometry of the GPS/WLAN (1.575/2.4/5.2/5.8 GHz) open-slot antenna with a sticker-like feed substrate for the metal-casing smartphone application. (b) The sticker-like feed substrate with the microstrip feedline and circuit elements disposed thereon. (c) Dimensions of the open slot in the metal casing. [Color figure can be viewed in the online issue, which is available at wileyonlinelibrary.com]

open-slot antenna can thus be obtained. For most cases, the open slot should be disposed in the metal casing with a distance less than about 10 mm to the short edge of the smartphone [11].

It is also noted that in order to have an attractive appearance of the metal casing, the open slot embedded therein should be simple and narrow in its structure, which makes it a design challenge to achieve multiband operation for the antenna to meet practical applications. In this study, a multiband open-slot antenna with a sticker-like feed substrate for the GPS (global positioning system) operation at 1.575 GHz [12–14] and WLAN (wireless wide area network) operation in the 2.4 GHz (2400–2484 MHz), 5.2 GHz (5150–5350 MHz), and 5.8 GHz (5725–5875 MHz) bands [15–18] is presented for the metal-casing smartphone application. The sticker-like feed substrate in this study is a 0.4-mm-thick FR4 substrate with the microstrip feedline and circuit elements disposed thereon. Note that in this study, the metal casing is with a simple rectangular shape, and the applied sticker-like feed substrate is a rigid FR4 substrate, although it has a thin thickness of 0.4 mm only. For practical applications, a flexible printed-circuit board (PCB) can be applied as the sticker-like feed substrate. In this case, when the smartphone is with a smoothly curved metal casing, the flexible PCB can have the conformal capability to be attached onto the inner surface of the metal casing easily, so as to excite the open slot embedded therein to be an efficient radiator.

In the proposed design, simply by attaching the sticker-like feed substrate onto a simple linear open slot embedded in the metal casing, the GPS/WLAN multiband operation can be obtained. The open slot has a small size of 1.5 mm in width and 23.5 mm in length and is spaced a short distance of 8 mm to the short edge of the metal casing, allowing it not to be covered by the display panel in the smartphone. With a narrow width, the open slot is also attractive to be embedded in the metal casing, so that the effects of its presence on the appearance of the smartphone can be decreased. The circuit elements include a shunt chip capacitor loaded across the open slot and a parallel chip capacitor added to the microstrip feedline. The circuit elements lead to multiband operation of the antenna, and its working principle will be addressed in this study. Experimental results of the proposed antenna are also presented and discussed.

2. ANTENNA STRUCTURE AND WORKING PRINCIPLE

2.1. Antenna Structure

Figure 1(a) shows the geometry of the GPS/WLAN (1.575/2.4/5.2/5.8 GHz) open-slot antenna with a sticker-like feed substrate for the metal-casing smartphone. The antenna is formed by attaching the sticker-like feed substrate [see Fig. 1(b)] onto the linear open slot in the metal casing [see Fig. 1(c)], with point *B* (*B*') at the side edge of the feed substrate fixed to point *A* (*A*') on the metal frame. The metal casing includes the rectangular metal backcover (width 76.6 mm and length 152.8 mm) and the metal frame (height 6 mm) disposed around the edges thereof. Note that only the metal frame at the top edge and two side edges is included in this study. The metal frame at the bottom edge is neglected for simplicity, which is expected to have negligible or no effects on the obtained results presented here. Also note that the metal backcover and the metal frame in the experimental study are fabricated using a double-side grounded FR4 substrate of thickness 0.8 mm. The printed ground planes on both surfaces are connected using adhesive copper foils at the edges so as to simulate a 0.8-mm-thick copper plate for the metal backcover and metal frame. In this case, the thickness of the smartphone is 6.8 mm, which includes 6-mm-wide metal frame and the 0.8-mm-thick metal backcover.

As shown in Figure 1(c), the open slot (slot portion DAC) is embedded in the metal casing, with the 1.5-mm slot opening (between point *C* and *C*') disposed at the metal frame. The open slot also has a narrow slot width of 1.5 mm and a short total length of 23.5 mm (17.5 mm on the metal backcover and 6 mm on the metal frame), which corresponds to only about 0.12 wavelength at 1.575 GHz, yet the antenna can generate its fundamental resonant mode at 1.575 GHz for the GPS operation. Note that since the open slot is embedded in the metal casing, it has a thickness of 0.8 mm and can be considered to have a 0.8-mm-thick FR4 substrate (relative permittivity 4.4 and loss tangent 0.02) filled therein. With the filled FR4 substrate as the dielectric loading, the resonant length of the open-slot antenna will hence be decreased. The linear open slot is also seen to have a short distance of 8 mm to the top edge of the metal casing, which allows the open slot not to be covered by the display panel in the smartphone.

For the sticker-like feed substrate shown in Figure 1(b), it has a printed 50-ohm microstrip feedline (width 0.75 mm) and the circuit elements of a shunt capacitor C_s (3.0 pF) and a parallel capacitor C_p (0.3 pF) disposed thereon. The microstrip

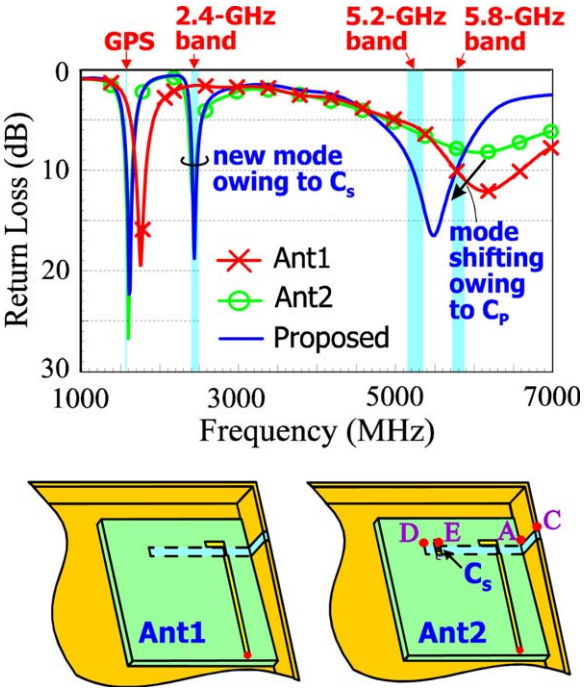

Figure 2 Simulated return loss for the proposed antenna, the case without C_s, C_p (Ant1), and Ant1 with C_s (Ant2). [Color figure can be viewed in the online issue, which is available at wileyonlinelibrary.com]

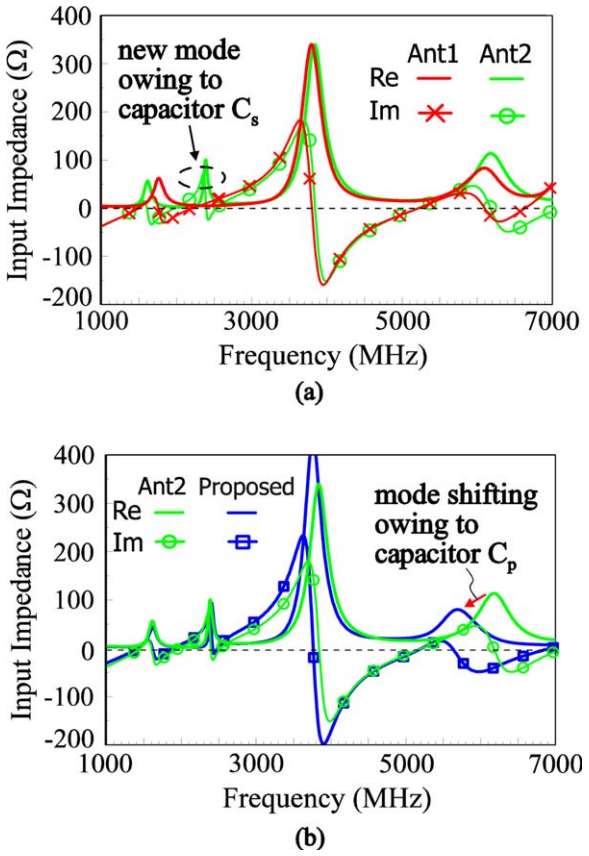

Figure 3 Simulated input impedance for (a) Ant1 and Ant2 and (b) Ant2 and proposed antenna. [Color figure can be viewed in the online issue, which is available at wileyonlinelibrary.com]

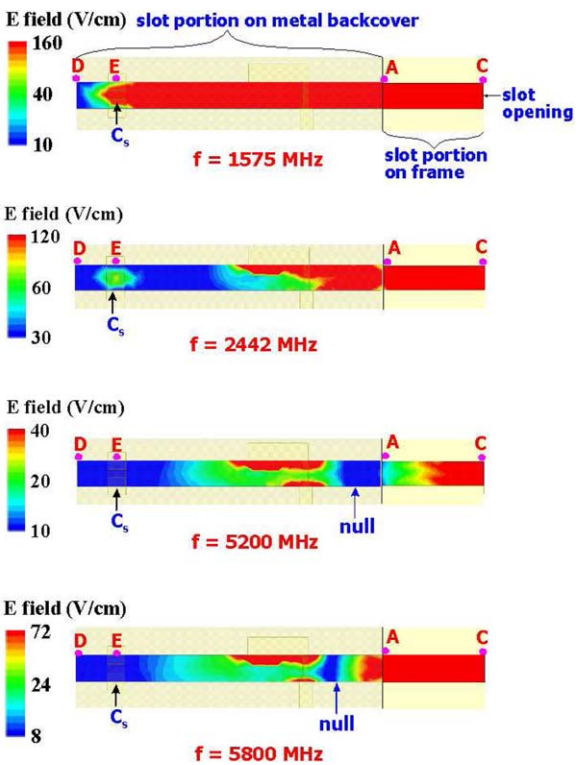

Figure 4 Simulated electric field distributions on the slot of the proposed antenna at 1575, 2442, 5200, and 5800 MHz. [Color figure can be viewed in the online issue, which is available at wileyonlinelibrary.com]

feedline has a narrow section of width 0.3 mm across the open slot and an open-ended tuning stub of length 3.5 mm. The narrow section contributes an additional inductance in the microstrip feedline and leads to a simplified matching network design for the proposed multiband antenna. A 0.4-mm-thick FR4 substrate is used as the feed substrate in the study. As mentioned earlier, a flexible PCB can also be applied as the feed substrate, which can make the feed substrate more suitable to be attached onto the open slot embedded in the metal casing with a smoothly curved surface. In this study, the metal backcover is selected to have a rectangular planar structure to simplify the experimental testing and the simulation study as well.

Both C_s and C_p are chip capacitors, and there are three vias in the feed substrate to connect them to the metal backcover when the feed substrate is attached onto the linear open slot. The capacitor C_s is loaded across the open slot at a distance of 15.2 mm to the metal frame, which can contribute to a new open-slot resonator created (slot portion EAC) and therefore generate a resonant mode for the 2.4-GHz WLAN operation. The capacitor C_p is connected as a parallel capacitor to the microstrip feedline and can fine-adjust the resonant frequency and widen the bandwidth of the higher-order mode of the open slot (slot portion DAC) to cover the 5.2/5.8-GHz WLAN operation. Details of the working principle of the antenna and the applied capacitors in the feed substrate are addressed in the following sections.

2.2. *Working Principle*

Figure 2 shows the simulated return loss for the proposed antenna, the case without C_s, C_p (Ant1), and Ant1 with C_s (Ant2). The simulated results are obtained using the high-frequency structure simulator HFSS version 15 [19]. The results for Ant1 show that a resonant mode at about 1.575 GHz is generated for the GPS signal reception. This resonant mode is the fundamental mode of the open-slot portion DAC and can be

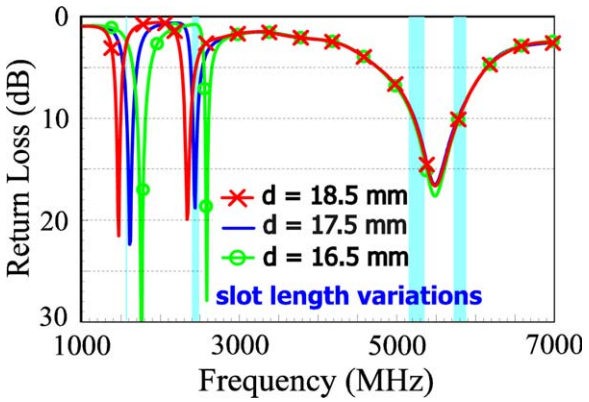

Figure 5 Simulated return loss as a function of the open-slot length d in the metal backcover. Other parameters are the same as given in Fig. 1. [Color figure can be viewed in the online issue, which is available at wileyonlinelibrary.com]

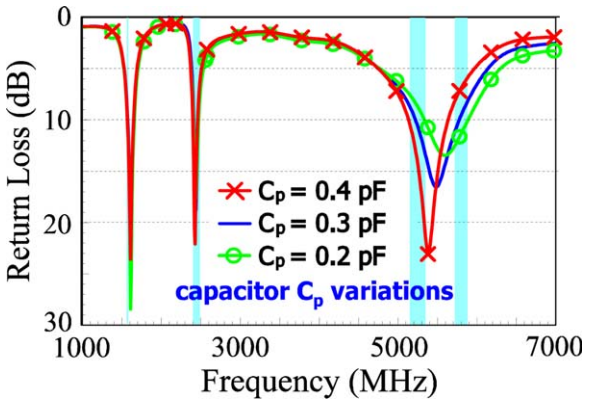

Figure 7 Simulated return loss as a function of the parallel capacitor C_p added to the microstrip feedline. Other parameters are the same as given in Fig. 1. [Color figure can be viewed in the online issue, which is available at wileyonlinelibrary.com]

confirmed by the simulated electric field distributions on the slot shown in Figure 4, which will be discussed later. When the shunt capacitor C_s is added to form Ant2, it is seen that a new resonant mode contributed by the open-slot portion EAC occurs to cover the 2.4-GHz WLAN band. For the parallel capacitor C_p added to the microstrip feedline of Ant2 to obtain the proposed antenna, it functions like a low-pass matching circuit to make the higher-order resonant mode of the open-slot portion DAC adjusted to cover the 5.2/5.8-GHz WLAN band, yet with very small effects on the first two resonant modes for the GPS and 2.4-GHz WLAN operation. In this case, the proposed antenna can cover the GPS/WLAN multiband (1.575/2.4/5.2/5.8 GHz) operation. It should also be noted that although the impedance matching for some frequencies at the band edges of the 5.2/5.8-GHz bands is slightly less than 10-dB return loss, the obtained antenna efficiencies are all better than 75%, which will be discussed with the aid of Figure 11 in Section 4.

Effects of the capacitors C_s and C_p can also be seen more clearly in Figure 3. In Figure 3(a), the simulated input impedance for Ant1 and Ant2 is shown. It is seen that an additional resonant mode is generated at about 2.4 GHz, owing to the presence of the capacitor C_s. While in Figure 3(b), the resonant mode at about 6.2 GHz is shifted to be at about 5.7 GHz, owing to the presence of the capacitor C_p. The combined effects of C_s and C_p thus make the antenna capable of covering the 2.4/5.2/5.8-GHz WLAN bands.

To further confirm the excited resonant modes in the proposed antenna, Figure 4 shows the simulated electric field distributions on the slot thereof. At 1575 MHz, the electric fields are uniformly excited in the slot from the slot coupling to near the closed end at point D, which indicates that the quarter-wavelength slot resonant mode contributed by the slot portion DAC is excited [5]. At 2442 MHz, it is observed that at point E, where the shunt capacitor C_s is located, some strong electric fields are generated. In addition, strong electric fields are also seen at the slot opening and then gradually decreased toward the capacitor C_s. This suggests that the capacitor C_s can function like a virtual shorting [20] to create a new open-slot portion EAC, and a new quarter-wavelength slot resonant mode contributed by the created open-slot portion can hence be generated. At 5200 and 5800 MHz, very weak electric fields are seen at point E, which indicates that the capacitor C_s has very small effects on the resonant modes excited in the 5-GHz band. It is also seen that there is a null field in the electric field distributions at 5200 and 5800 MHz. This indicates that the excited resonant mode at 5200 and 5800 MHz is a higher-order resonant mode of the open-slot portion DAC. The observed electric field distributions agree with the return-loss results seen in Figures 2 and 3.

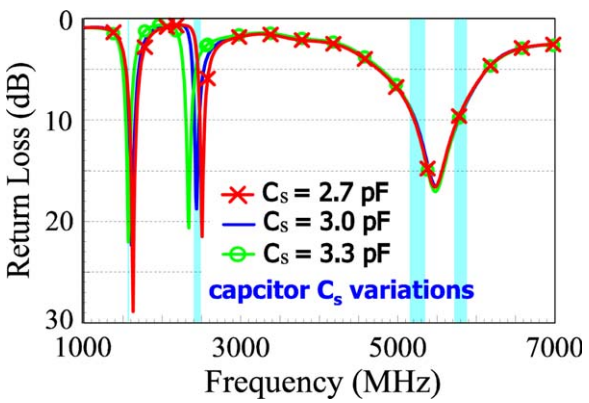

Figure 6 Simulated return loss as a function of the shunt capacitor C_s across the slot. Other parameters are the same as given in Fig. 1. [Color figure can be viewed in the online issue, which is available at wileyonlinelibrary.com]

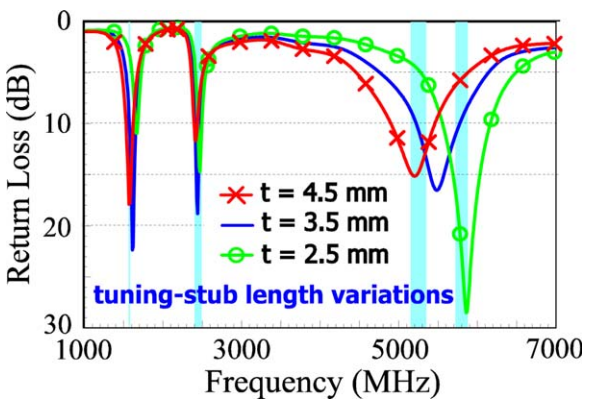

Figure 8 Simulated return loss as a function of the tuning-stub length t for the proposed antenna. Other parameters are the same as given in Fig. 1. [Color figure can be viewed in the online issue, which is available at wileyonlinelibrary.com]

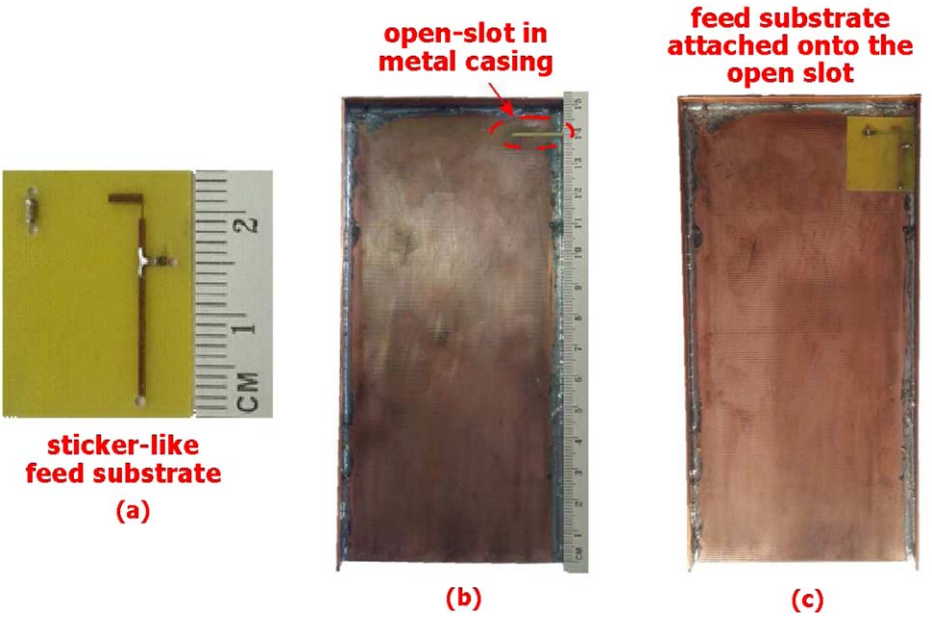

Figure 9 Photos of the fabricated antennas. (a) The sticker-like feed substrate. (b) The metal casing with the open-slot embedded therein. (c) The feed substrate attached on the open slot in the metal casing. [Color figure can be viewed in the online issue, which is available at wileyonlinelibrary.com]

Also note that the proposed antenna at 1575 MHz radiates a linearly polarized wave. Although the GPS radiation uses the right-hand circularly polarized wave [12–14], the linearly polarized antenna has been widely used for the GPS signal reception in the smartphone [12]. This is mainly because the orientation of the smartphone is generally not fixed, which is dependent on how the user holding the same. In this case, the circularly polarized antenna is not advantageous over the linearly polarized antenna in the GPS signal reception. Hence, for the modern smartphone, the linearly polarized antenna has been generally applied for the GPS operation.

3. PARAMETRIC STUDY

Some parameters of the proposed antenna in controlling the multiband operation are studied in this section. Figure 5 shows the simulated return loss as a function of the length d of the open-slot portion DEA in the metal backcover. Other parameters are fixed and the same as given in Figure 1. The simulated results for the length d varied from 16.5 to 18.5 mm are presented. The first two modes of the antenna are seen to be shifted to lower frequencies with an increase in the length d. This is reasonable, since the increase in the slot length will result in a longer resonant length, thereby decreasing the resonant frequencies of the excited resonant modes. However, it is interesting to note that the higher-order mode in the 5.2/5.8-GHz bands is very slightly affected. This implies that the length variation is effective in causing effects on the fundamental mode, but not the higher-order mode.

Figure 6 shows the simulated return loss as a function of the shunt capacitor C_s across the slot. Results of the capacitor C_s varied from 2.7 to 3.3 pF are shown. Significant effects on the second mode for the 2.4-GHz band are seen, with relatively small effects seen for the other two modes. This is largely

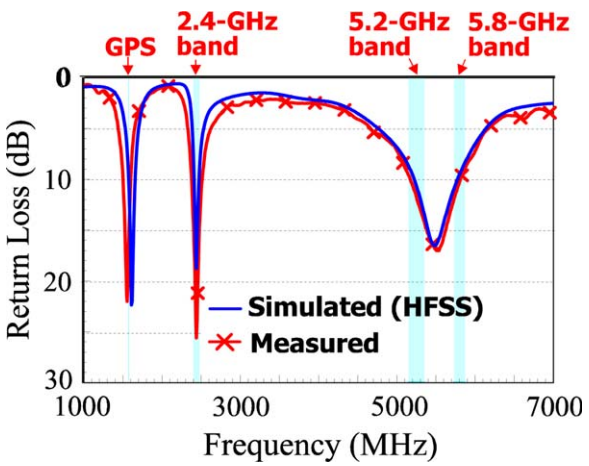

Figure 10 Measured and simulated return losses for the fabricated antenna. [Color figure can be viewed in the online issue, which is available at wileyonlinelibrary.com]

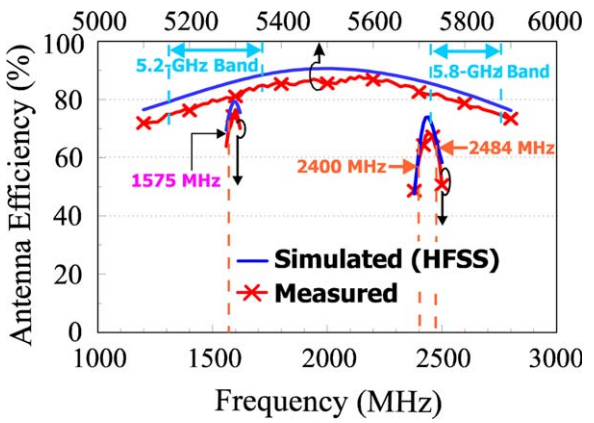

Figure 11 Measured and simulated antenna efficiencies for the fabricated antenna. [Color figure can be viewed in the online issue, which is available at wileyonlinelibrary.com]

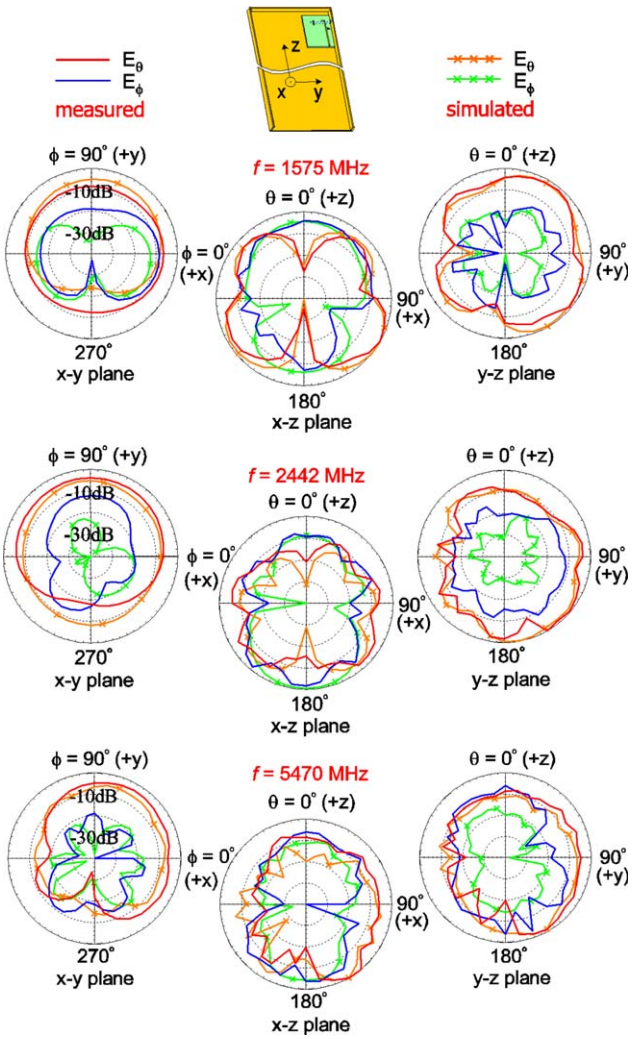

Figure 12 Measured and simulated radiation patterns for the fabricated antenna. [Color figure can be viewed in the online issue, which is available at wileyonlinelibrary.com]

because the capacitor C_s controls the generation of the second mode. Moreover, with a larger value of the capacitor C_s, a smaller capacitive reactance is obtained [21], which can lead to an increased effective length of the created slot portion EAC and its corresponding resonant mode is therefore shifted to lower frequencies. Hence, by tuning the capacitor C_s, the resonant mode for the 2.4-GHz band can be fine-adjusted.

Figure 7 shows the simulated return loss as a function of the parallel capacitor C_p added to the microstrip feedline. Results of the capacitor C_p varied from 0.2 to 0.4 pF are shown. In this case, significant effects on the third mode for the 5.2/5.8-GHz bands are seen, with the first two modes relatively very slightly affected. That is, the capacitor C_p can be tuned to effectively control the occurrence of the third mode (the higher-order mode of the open-slot portion DAC) to cover the 5.2/5.8-GHz bands.

Effects of varying the tuning-stub length t on the excited resonant modes of the antenna are also studied. Figure 8 shows the simulated return loss for the length t varied from 2.5 to 4.5 mm. In this case, the third mode for the 5.2/5.8-GHz bands can also be adjusted, with the other two modes relatively slightly affected. This is largely because the variations in the tuning-stub length mainly cause some variations in the imaginary part of the input impedance and will effectively shift the resonant frequency with zero reactance, and the higher-order mode is generally more sensitive to the variations of the same. Hence, with the tuning-stub length variations, significant effects on the third mode are observed.

4. EXPERIMENTAL RESULTS

The proposed antenna was fabricated, and its photos are shown in Figure 9. The sticker-like feed substrate and the metal casing with an open slot embedded therein are respectively shown in Figures 9(a) and 9(b). The fabricated antenna with the feed substrate attached onto the open slot is shown in Figure 9(c). The measured and simulated return losses for the fabricated antenna are presented in Figure 10. Fair agreement between the simulated results and the measured data is observed. The experimental results indicate that the proposed antenna can cover the 1.575/2.4/5.2/5.8-GH multiband operation.

The fabricated antenna was also tested in a far-field anechoic chamber. The measured and simulated antenna efficiencies are presented in Figure 11. Reasonable agreement between the measurement and simulation is also seen. The measured antenna efficiencies with the mismatching losses included are about 70% for the GPS operation at 1.575 GHz, about 57–66% for the 2.4-GHz WLAN operation, and better than 75% for the 5.2/5.8-GHz WLAN operation. The obtained antenna efficiencies are acceptable for practical applications.

Figure 12 shows the measured and simulated radiation patterns for the fabricated antenna. Results of three frequencies at 1575, 2442, and 5470 MHz are plotted. The latter two frequencies are at about the central frequencies of the excited resonant modes for the 2.4-GHz and 5.2/5.8-GHz WLAN bands. The measured radiation patterns are in fair agreement with the simulated results. At 1575 MHz, stronger radiation in the $+y$ direction is seen in the x–y plane (azimuthal plane) and the y–z plane (elevation plane parallel to the metal casing), which is largely because the antenna is disposed at the right-hand-side metal frame in this study. Similarly, stronger radiation in the $+y$ direction is observed at 2442 and 5470 MHz. For practical applications, a second WLAN antenna can be disposed at the left-hand-side metal frame for the MIMO (multi-input multi-output) or diversity operation [22,23]. In this case, it is expected that the radiation pattern of the second WLAN antenna will be stronger in the $-y$ direction, which will be advantageous to achieve good independent or diversity patterns of the two antennas. In addition, owing to the large distance between the two side edges of the smartphone, good isolation between the two such antennas can be expected. That is, the proposed antenna is promising for practical applications, including the MIMO and diversity operations, in the smartphone.

5. CONCLUSION

A design of using a sticker-like feed substrate to feed a simple linear open slot embedded in the metal casing of the smartphone to achieve multiband operation has been proposed. The antenna in this study can have the multiband (1.575/2.4/5.2/5.8 GHz) operation for the GPS/WLAN operation, although it has a short length of only about 0.12 wavelength at 1575 MHz. Working principle of the multiband operation using the circuit elements (a shunt capacitor across the slot and a parallel capacitor to the microstrip feedline) disposed on the sticker-like feed substrate has been described. Good radiation characteristics for frequencies in the GPS/WLAN bands have also been observed. The antenna is promising for applications in the modern metal-casing smartphone with either a planar or smoothly curved surface.

REFERENCES

1. H. Wang, M. Zheng, and S.Q. Zhang, Monopole slot antenna, U.S. Patent No. 6618020 B2, 2003.
2. C.I. Lin and K.L. Wong, Printed monopole slot antenna for internal multiband mobile phone antenna, IEEE Trans Antennas Propag 55 (2007), 3690–3697.
3. Z. Liu and K. Boyle, Bandwidth enhancement of a quarter-wavelength slot antenna by capacitive loading, Microwave Opt Technol Lett 51 (2009), 2114–2116.
4. K.L. Wong, P.W. Lin, and C.H. Chang, Simple printed monopole slot antenna for penta-band WWAN operation in the mobile handset, Microwave Opt Technol Lett 53 (2011), 1399–1404.
5. K.L. Wong and C.Y. Tsai, Low-profile dual-wideband inverted-T open slot antenna for the LTE/WWAN tablet computer with a metallic frame, IEEE Trans Antennas Propag 63 (2015), 2879–2886.
6. T.Y. Kim, C.H. Yang, I.Y. Lee, and S.H. Choi, Case and electronic apparatus, U.S. Patent Application Publication No.: 2014/0218250 A1, Aug. 7, 2014.
7. T.H. Tsai, C.P. Chiu, W.Y. Wu, and H.W. Wu, Mobile device and antenna structure therein, U.S. Patent Application Publication No.: 2014/0062815 A1, Mar. 6, 2014.
8. R.J. Hill, R.W. Schlub, and R. Caballero, Parallel-fed equal current density dipole antenna, U.S. Patent No. 8368602 B2, Feb. 5, 2013.
9. J. Zhong, K.K. Chen, and X. Sun, A novel multi-band antenna for mobile phone with metal frame, 2012 International Conference on Wireless Communications, Networking and Mobile Computing, Shanghai, China, pp. 1–4.
10. K.L. Wong and P.R. Wu, Low-profile dual-wideband dual-inverted-L open-slot antenna for the LTE/WWAN tablet device, Microwave Opt Technol Lett 57 (2015), 1813–1818.
11. K.L. Wong and P.R. Wu, Dual-wideband linear open slot antenna with two open ends for the LTE/WWAN smartphone, Microwave Opt Technol Lett 57 (2015), 1269–1274.
12. Y. Li, Z. Zhang, J. Zheng, Z. Feng, and M.F. Iskander, A compact hepta-band loop-inverted F reconfigurable antenna for mobile phone, IEEE Trans Antennas Propag 60 (2012), 389–392.
13. C.M. Su and K.L. Wong, A dual-band GPS microstrip antenna, Microwave Opt Technol Lett 33 (2002), 238–240.
14. C.M. Su and K.L. Wong, Surface-mountable dual side-feed circularly polarized ceramic chip antenna for GPS operation, Microwave Opt Technol Lett 35 (2002), 137–138.
15. K.L. Wong, H.J. Jiang, and Y.C. Kao, High-isolation 2.4/5.2/5.8 GHz WLAN MIMO antenna array for laptop computer application, Microwave Opt Technol Lett 55 (2013), 382–387.
16. T.W. Kang and K.L. Wong, Isolation improvement of 2.4/5.2/5.8 GHz WLAN internal laptop computer antennas using dual-band strip resonator as a wavetrap, Microwave Opt Technol Lett 52 (2010), 58–64.
17. S.W. Su, High-gain dual-loop antennas for MIMO access points in the 2.4/5.2/5.8 GHz bands, IEEE Trans Antennas Propag 58 (2010), 2412–2419.
18. J.H. Yoon and Y.C. Lee, Modified bow-tie slot antenna for the 2.4/5.2/5.8 GHz WLAN bands with a rectangular tuning stub, Microwave Opt Technol Lett 53 (2011), 126–130.
19. Available at: http://www.ansys.com/products/hf/hfss/, ANSYS HFSS.
20. N. Behdad and K. Sarabandi, A multiresonant single-element wideband slot antenna, IEEE Antennas Wireless Propag Lett 3 (2004), 5–8.
21. K.L. Wong and Z.G. Liao, Passive reconfigurable triple-wideband antenna for LTE tablet computer, IEEE Trans Antennas Propag 63 (2015), 901–908.
22. T.Y. Wu, S.T. Fang, and K.L. Wong, Printed diversity dual-band monopole antenna for WLAN operation, Microwave Opt Technol Lett 36 (2003), 436–439.
23. K.L. Wong and J.Y. Lu, 3.6-GHz 10-antenna array for MIMO operation in the smartphone, Microwave Opt Technol Lett 57 (2015), 1609–1704.

A NOVEL TEXTILE ANTENNA USING COMPOSITE MULTIFILAMENT CONDUCTIVE THREADS FOR SMART CLOTHING APPLICATIONS

Jian-Syuan Huang, Tong-Yang Jiang, Zhi-Xiang Wang, Sheng-Wei Wu, and Yen-Sheng Chen
Department of Electronic Engineering, National Taipei University of Technology, Taipei 10608, Taiwan, Republic of China;
Corresponding author: yschen@ntut.edu.tw

Received 31 August 2015

ABSTRACT: *This letter proposes a wearable antenna fabricated by multifilament threads. The radiator is conductive threads filled with a copper wire, directly sewn onto a piece of cloth. Its advantages include better impedance matching, enhanced radiation efficiency, and additional value to smart clothing because the radiator is shaped into a logotype.* © 2016 Wiley Periodicals, Inc. Microwave Opt Technol Lett 58:1232–1236, 2016; View this article online at wileyonlinelibrary.com. DOI 10.1002/mop.29771

Key words: *antennas; electronic textiles; monopole antennas; smart clothing*

1. INTRODUCTION

Recently, there has been increasing research interest in wearable communication systems, and the emergent technology has been deployed in various applications. Among these applications, smart clothing has gathered great importance over the past few years because it offers personal healthcare at home. With the increasing usage of smart clothing applications, reliability requirements for wireless communication have become more critical. Conventionally, the Bluetooth/WiFi modules of smart clothing applications use either on-chip antennas [1,2] or printed-circuit-board (PCB) antennas [3] to transmit the fitness data. However, these types of antennas result in lower reliability due to two limitations. For one thing, the input resistance of chip antennas and PCB antennas within a small area are found to be around 10 Ω, resulting in poorer impedance matching [4,5]; as a result, the input power of the antenna may be insufficient unless an external matching circuit is added. For another, the radiation efficiency of on-chip antennas and PCB antennas is usually very small. Because of the space constraint of the Bluetooth/WiFi modules, the size of these antennas must be miniaturized. However, a compact antenna structure requires a highly meander wire path, so the currents on the adjacent horizontal segments have opposite phase; thus, these transmission-line-wise currents do not give valuable contribution to the radiated power, so the radiation efficiency is greatly reduced. In addition, neither on-chip antennas nor PCB antennas are specially designed for smart clothing applications. They are usually fabricated on a FR4 substrate, which means that the environment of cloth is not well exploited.

The purpose of this letter is to present a novel antenna structure directly sewn onto a piece of cloth; more importantly, the proposed antenna has much better impedance matching and enhanced radiation efficiency as compared to on-chip antennas and PCB antennas. The radiator of this antenna is composite electro-conductive fabrics, which are very different from the textile radiators in the literature. The early development of textile radiators was conductive nylon fabrics or electro threads [6,7], the conductivity of which ranges between 10^3 S m^{-1} and 10^5 S m^{-1}. In this work, a thin copper wire is filled into the